

Review

Not peer-reviewed version

---

# PPO Inhibitors as a Key Focus in Herbicide Discovery

---

Min Zhao <sup>†</sup>, [Baojian Li](#) <sup>†</sup>, [Ying Gao](#), Rui Zhang, Subinur Ahmattohti, [Jie Li](#) <sup>\*</sup>, [Xinbo Shi](#) <sup>\*</sup>

Posted Date: 3 March 2026

doi: 10.20944/preprints202603.0110.v1

Keywords: PPO inhibitors; herbicide discovery; molecular design



Preprints.org is a free multidisciplinary platform providing preprint service that is dedicated to making early versions of research outputs permanently available and citable. Preprints posted at Preprints.org appear in Web of Science, Crossref, Google Scholar, Scilit, Europe PMC.

Copyright: This open access article is published under a [Creative Commons CC BY 4.0 license](#), which permit the free download, distribution, and reuse, provided that the author and preprint are cited in any reuse.

Disclaimer/Publisher's Note: The statements, opinions, and data contained in all publications are solely those of the individual author(s) and contributor(s) and not of MDPI and/or the editor(s). MDPI and/or the editor(s) disclaim responsibility for any injury to people or property resulting from any ideas, methods, instructions, or products referred to in the content.

Review

# PPO Inhibitors as a Key Focus in Herbicide Discovery

Min Zhao <sup>1,†</sup>, Baojian Li <sup>1,2,†</sup>, Ying Gao <sup>1,2</sup>, Rui Zhang <sup>1,2</sup>, Subinur Ahmattohti <sup>1</sup>, Jie Li <sup>1,\*</sup> and Xinbo Shi <sup>3,\*</sup>

<sup>1</sup> School of Pharmacy, Xinjiang Second Medical College, Karamay 834000, China

<sup>2</sup> Science and Innovation Center of Xinjiang Second Medical College, Karamay 834000, China

<sup>3</sup> Shaanxi Collaborative Innovation Center of Chinese Medicine Resources Industrialization, Shaanxi University of Chinese Medicine, Xianyang 712046

\* Correspondence: lijie@xjsmc.edu.cn (J.L.); 1501026@sntcm.edu.cn (X.S.)

† These authors contributed equally to this work.

## Abstract

As the key enzyme catalyzing the final step in the biosynthesis of heme and chlorophyll, protoporphyrinogen oxidase (PPO) has become a crucial target for herbicide development. To date, more than 40 PPO-inhibiting herbicides have been developed, exhibiting multiple advantageous characteristics: they combine high efficacy with environmental friendliness, feature low effective concentrations, rapid action, long-lasting effects, and excellent control of both monocotyledonous and dicotyledonous weeds. In recent years, significant progress has been made in the structural biology of PPO—five crystal structures from tobacco, humans, and various bacteria have been resolved, most of which are presented as enzyme-inhibitor complexes. Although the development of such herbicides spans over five decades, novel PPO inhibitors still hold broad potential for innovation due to the resistance of early applied PPOs. This review systematically summarizes the three-dimensional structures of PPO from different sources, the interaction mechanisms between the enzyme and inhibitors, studies on quantitative structure-activity relationships of inhibitors, and outlines molecular design directions for the next generation of PPO inhibitors.

**Keywords:** PPO inhibitors; herbicide discovery; molecular design

## 1. Introduction

Protoporphyrinogen oxidase (PPO; EC 1.3.3.4) serves as the final shared catalytic component within the biosynthetic routes that produce both chlorophyll and heme [1]. This membrane-associated enzyme family exhibits high evolutionary conservation and is present across diverse taxa, including bacteria, fungi, plants, and mammals. During the reaction, PPO facilitates the six-electron oxidation of protoporphyrinogen-IX into the fully conjugated macrocycle known as protoporphyrin IX in a molecular oxygen-dependent environment (Figure 1). Within plant systems, PPO exists as two distinct isoforms: the mitochondrial PPO2 and the plastid PPO1 [2]. Specifically, PPO1 is integrated into the chloroplast envelope and thylakoid membranes, whereas PPO2 is localized on the outer surface of the inner mitochondrial membrane.

The metabolic disorder known as variegated porphyria (VP) is a dominant hereditary condition arising from pathogenic variations within the human PPO gene. Clinically, VP is characterized by neurological manifestations, acute abdominal distress, and dermal photosensitivity [3-5]. This condition exhibits a higher prevalence among females than males and can manifest abruptly at any life stage, ranging from adolescence to late adulthood [6]. Research indicates that patients diagnosed with VP typically demonstrate a minimum 50% reduction in PPO enzymatic activity [7]. Such enzymatic impairment, often triggered by specific amino acid substitutions near the active site

(notably the R59W mutation), results in the systemic accumulation of protoporphyrin IX, thereby heightening light sensitivity in affected individuals.

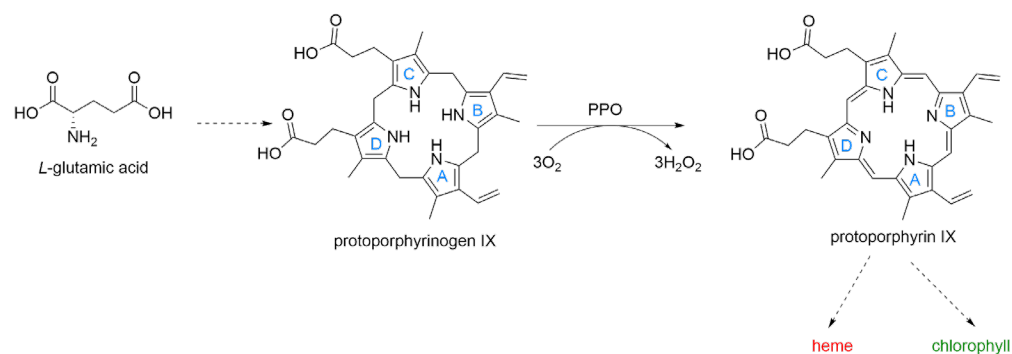


**Figure 1.** Protoporphyrinogen oxidase (PPO) catalyzes the enzymatic reaction converting protoporphyrinogen IX to protoporphyrin IX, the penultimate step in porphyrin biosynthesis. Solid arrows indicate single enzymatic steps, dashed arrows indicate multiple enzymatic steps.

Furthermore, scientific focus on PPO has expanded considerably following the discovery of its therapeutic potential in cancer management via photodynamic therapy (PDT) [8]. Specifically, Halling and colleagues [9] established that PPO inhibitors can induce the targeted buildup of photosensitizing protoporphyrinogen-IX within malignant cells.

In botanical science, PPO is recognized as a critical molecular target for a wide range of structurally heterogeneous herbicides. This diverse group encompasses chemical families such as diphenylethers [10], phenylpyrazole [11], oxadiazoles [12], triazolinones [13], thiadiazoles [14], pyrimidindiones [15], oxazolidinediones [16], and *N*-phenylphthalimides [17], among various other classes [18].

The pharmacological interference with this plant enzyme initiates a pathological cascade, beginning with the intracellular surge of the substrate protoporphyrinogen-IX. This accumulated precursor is subsequently translocated to the cytosol, where it undergoes spontaneous, non-catalytic oxidation driven by molecular  $O_2$  within the vicinity of mitochondria and chloroplasts [19]. This reaction yields a photo-reactive variant of protoporphyrin IX. Upon exposure to solar radiation, this intermediate facilitates the generation of singlet oxygen, a highly reactive species that precipitates lethal lipid peroxidation and eventual cellular collapse. Consequently, these PPO-targeting compounds are formally categorized as light-dependent bleaching herbicides [20].

The present review aims to synthesize the prevailing understanding of PPO structural characteristics across various species, specifically focusing on human, bacterial, and botanical sources. Furthermore, it elucidates the complex binding modalities between PPOs and their inhibitors, alongside an exploration of the quantitative structure-activity relationships (QSARs) that define these chemical interactions. Finally, the article details the rational molecular design principles that have underpinned the development of contemporary commercial PPO inhibitors.

## 2. Structure of PPOs

Deciphering the spatial architecture of an enzyme is essential for elucidating catalytic pathways, mapping inhibitor-enzyme associations, and facilitating rational drug discovery. In 2004, the inaugural crystal structure of tobacco-derived mitochondrial PPO2 (mtPPO) was characterized by Koch et al. [21], revealing its complex with the inhibitor INH (fluazolate, see **Figure**). This dimeric, yellow-pigmented protein was resolved at 2.9 Å using selenium-based single anomalous diffraction. Its molecular scaffold comprises three distinct regions: an  $\alpha$ -helical domain responsible for membrane attachment; a FAD-binding domain resembling the topology of *p*-hydroxybenzoate hydroxylase; and a substrate-binding domain housing a constricted active site beneath the FAD cofactor.

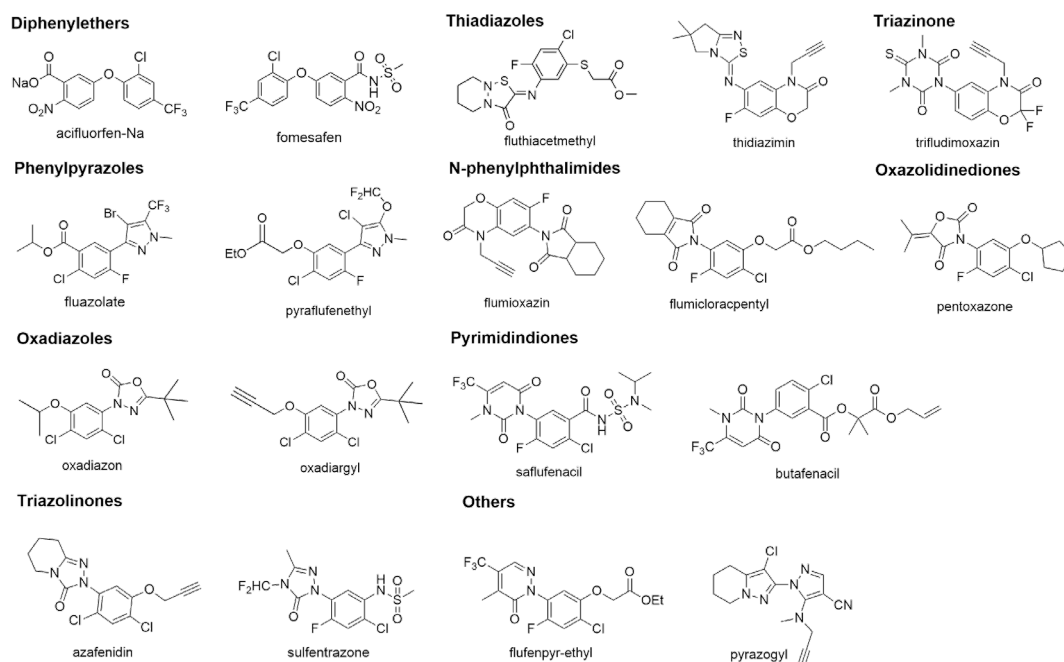


**Figure 2.** Chemical structures of selected representative protoporphyrinogen oxidase-inhibiting herbicides.

Subsequent crystallographic studies expanded this structural library to include bacterial PPO from *Myxococcus xanthus* (mxPPO) [22], *Bacillus subtilis* (bsPPO) [23], and the human ortholog (hPPO) [24], typically studied in complex with acifluorfen (Figure 2). While mtPPO, mxPPO, and hPPO function as membrane-associated dimers sensitive to diphenylether herbicides, bsPPO represents a distinct outlier within this enzyme family. Notably, bsPPO is a soluble, monomeric protein that possesses a more expansive substrate range and exhibits resistance to AF inhibition.

Sequence alignment reveals that mtPPO, mxPPO, bsPPO, and hPPO exhibit minimal primary sequence identity. Nevertheless, these enzymes share remarkably congruent global folding patterns, as characterized by Koch et al. [21]. Their structural framework consistently integrates three functional domains: an FAD-binding domain, a substrate-binding domain, and a membrane-binding domain. Specifically, the FAD-binding region demonstrates substantial structural and sequence homology with the broader flavoenzyme family.

The high degree of structural conservation is further evidenced by the superimposition of the mtPPO substrate-binding domain onto those of mxPPO, bsPPO, and hPPO, yielding root-mean-square deviations (RMSD) for  $C_{\alpha}$  atoms of 0.7 Å, 1.1 Å, and 0.8 Å, respectively. Apart from minor variations in specific loop regions—likely stemming from evolutionary insertions or deletions—the conformations of the substrate-binding and FAD-binding domains across these four enzymes are nearly indistinguishable [22–24].

In stark contrast, the membrane-binding domains display significant conformational divergence, which is presumably dictated by their distinct lipid-interaction mechanisms. For instance, crystallographic analysis suggests that mtPPO associates with the membrane as a homodimer [21], whereas mxPPO does not form a physiologically active dimeric state. Instead, for mxPPO, the hydrophobic interface comprising helices 4, 5, and 10 within its membrane-binding domain is proposed to function as a specialized membrane anchor [22].

The PPO catalytic center is a hydrophobic pocket situated at the junction of the substrate-binding and FAD-binding domains, housing a suite of functionally significant and evolutionarily conserved residues [21–24]. As illustrated in **Figure**, the most invariant of these is a glycine residue (identified as Gly175 in mtPPO, Gly167 in mxPPO, Gly169 in hPPO, and Gly175 in bsPPO). The carbonyl oxygen of this glycine extends from the base of the pocket toward the center of the active site, where it facilitates interactions with the tetrapyrrole macrocyclic framework.

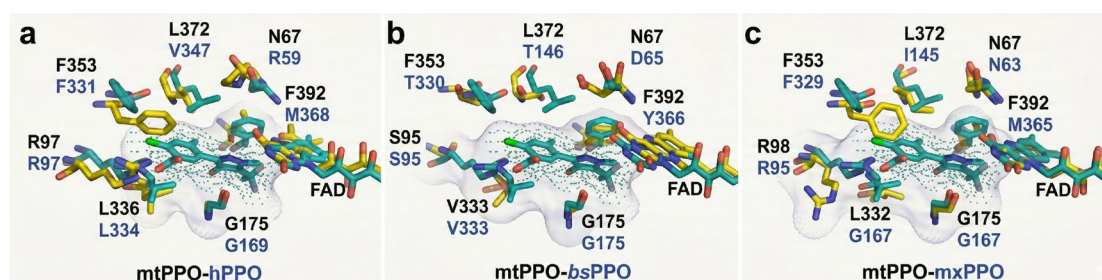


**Figure 3.** The active sites of PPOs. (a) Mitochondrial and human PPOs (mtPPO-hPPO); (b) mitochondrial and bacterial PPOs (mtPPO-bsPPO); (c) Mitochondrial and bacterial PPOs (mtPPO-mxPPO).

Another prominent conserved residue is the arginine located at positions 98, 95, and 97 in mtPPO, mxPPO, and hPPO, respectively; notably, this position is occupied by Ser95 in the bsPPO ortholog. Based on substrate-bound structural simulations, this residue is thought to engage in ionic interactions or hydrogen bonding with the C-ring propionic acid group. The consistent presence of this bulky side chain on one side of the binding pocket appears to impose steric constraints on the opposing side, which invariably accommodates smaller, uncharged residues such as Ala, Gly, Thr, or Ser. Furthermore, a third highly conserved site is occupied by Phe353 (corresponding to Phe329 in mxPPO, Phe331 in hPPO, and Thr330 in bsPPO). This residue is strategically positioned to define the vertical clearance of the cavity ceiling relative to the FAD macrocycle.

**Figure** further delineates additional pivotal residues within the active site which, despite lacking high evolutionary conservation, exhibit comparable steric or chemical characteristics across diverse PPO species. A notable example is the stacking interaction with ring A of protoporphyrinogen-IX, mediated by Phe392 in mtPPO [21], a position occupied by Met365 and Tyr366 in mxPPO and bsPPO, respectively. Similarly, the position adjacent to the FAD isoalloxazine ring shows significant variability: the Asn67 found in mtPPO is replaced by Asn63 in mxPPO, Asp65 in bsPPO, and Arg59 in hPPO.

This human-specific Arg59 has garnered extensive research interest due to its indispensable role in sustaining enzymatic functionality and structural equilibrium *in vitro*. Before the definitive resolution of the hPPO crystal structure, computational models based on mtPPO suggested that Arg59 formed a critical salt bridge with Asp349, thereby preserving the active site's structural framework. Among various pathological variants, the R59W mutation is the most frequently analyzed, given its strong correlation with Variegated Porphyria (VP). Crystallographic evidence presented by Qin et al. [24] reveals that the hydrophilic binding environment actively repels the hydrophobic indolyl ring of the substituted tryptophan. This repulsion severely undermines the necessary interaction between the FAD isoalloxazine ring and the incoming substrate.

Additionally, the binding pocket utilizes a pair of variable residues to stabilize the substrate's B ring through hydrophobic "sandwiching." This structural motif is formed by Leu356 and Leu372 in mtPPO, Leu332 and Ile345 in mxPPO, Val333 and Thr346 in bsPPO, and Leu334 and Val347 in hPPO.

Notably, the diversity in substrate selectivity observed across various PPO orthologs is primarily attributed to significant variations in the dimensions of their respective binding pockets. Investigations by Qin and colleagues [23,24] quantified the internal volumes of these cavities, reporting 1,173 Å<sup>3</sup> for bsPPO, 440 Å<sup>3</sup> for mtPPO, and 627 Å<sup>3</sup> for mxPPO. Consequently, the pocket within bsPPO is capable of housing substrates that are twofold to threefold larger than those accommodated by either mtPPO or mxPPO. Furthermore, distinct electrostatic properties were identified within the bsPPO substrate-binding chamber, where the interior surface is characterized by a lining of positive charges—a feature noticeably absent in the binding environments of mtPPO and mxPPO. These combined structural and electronic factors likely underpin the enhanced substrate versatility characteristic of bsPPO relative to other members of the PPO enzyme family.

Currently, the definitive binding configuration of protoporphyrinogen-IX remains elusive, primarily because a crystal structure of PPO complexed with its native substrate or related structural analogs has yet to be resolved. Utilizing the mtPPO-inhibitor (INH) complex as a structural proxy, Koch and associates [21] formulated the initial comprehensive binding model for the substrate. Their findings suggest that the two anionic propionyl moieties are oriented toward the solvent-accessible

regions of the pocket, with the C-ring propionyl group establishing an ionic bridge with the invariant Arg98. Furthermore, the A ring participates in  $\pi$ - $\pi$  stacking with Phe392, while the B ring is sequestered between the conserved residues Leu356 and Leu372.

This spatial arrangement aligns the C20 methylene bridge—which connects the A and D rings—in close proximity to the reactive N5 position of the FAD cofactor, supporting the hypothesis of a triphasic oxidation pathway [21]. A central feature of this proposed mechanism is that hydride abstraction consistently occurs at the C20 position of the tetrapyrrole framework, mediated by hydrogen rearrangements via imine-enamine tautomerization. Although this model has gained broad consensus, several fundamental ambiguities persist. For instance, while protoporphyrinogen-IX undergoes spontaneous oxidation by O<sub>2</sub>, the rate-limiting step of this non-catalytic transformation—and the precise divergence between enzymatic and non-enzymatic pathways—remains to be elucidated. Additionally, it remains undetermined whether the overall reaction rate is governed by substrate association or product dissociation kinetics.

Existing inhibitors typically function by emulating specific structural motifs of the native substrate, thereby engaging in competitive binding. Intriguingly, these agents employ diverse modes of molecular mimicry, and even a single inhibitor may exhibit ortholog-specific binding configurations across different species. For instance, INH serves as a structural analog for rings A and B of protoporphyrinogen-IX, with its carboxylate moiety effectively substituting for the propionate group attached to ring C [21].

Crystallographic evidence further highlights this variability; acifluorfen replicates the conformation of rings A and B in both mxPPO and hPPO [22,23], yet it aligns with the geometry of rings C and D when associated with bsPPO [24]. These observations imply that the combined binding profiles of two acifluorfen molecules can encompass the entire tetrapyrrole framework of the substrate. This conceptualization of "dual-mimicry" offers significant directions for the rational synthesis of PPO inhibitors.

### 3. PPO Inhibitors as a Key Focus Herbicides

Research into PPO-targeting herbicides has persisted for over six decades, though their specific pharmacological mechanisms remained obscure until the mid-1980s. Compared to alternative weed-control agents, PPO inhibitors present numerous strategic advantages, such as minimal toxicological impact and exceptional efficacy at modest application rates (10–50 g.ai/ha). Furthermore, they demonstrate a comprehensive herbicidal spectrum encompassing both monocotyledonous and dicotyledonous species, alongside a rapid onset of activity—often inducing necrosis within 24 hours—and sustained residual effectiveness.

Owing to these environmentally benign characteristics, several structural classes have been successfully commercialized over the past several decades. These include diphenylethers [10], phenylpyrazole [11], oxadiazoles [12], triazolinones [13], thiadiazoles [14], pyrimidindiones [15], oxazolidinediones [16], and *N*-phenylphthalimides [17]. Representative examples of these commercial PPO-inhibiting compounds are detailed in **Figure** [10].

In comparison to various other herbicidal categories, the emergence of resistance to PPO-inhibiting compounds has proceeded at a notably protracted pace. Despite their introduction to the commercial market in the 1960s, documented resistance has been confined to few weed species to date [25]. Among these, *Amaranthus tuberculatus*—a primary agricultural threat in the Midwestern United States—was first identified in 2001 as exhibiting cross-resistance to both PPO and acetohydroxamic synthase (AHAS) inhibitors. This resistance profile was subsequently observed in three additional dicot species: *Euphorbia heterophylla*, *A. quitensis*, and *Ambrosia artemisiifolia*.

Interestingly, the rise of PPO resistance is partially linked to the prior management of AHAS-resistant populations [26], as practitioners pivoted to PPO inhibitors to control weeds that no longer responded to AHAS-targeting chemistries. For instance, certain *A. tuberculatus* biotypes now resist PPO inhibitors such as lactofen and fomesafen, alongside AHAS inhibitors like imazethapyr and chlorimuron-ethyl.

Patzoldt et al. [27] identified that resistance within natural *A. tuberculatus* populations is conferred by a specific Gly210 codon deletion in the PPX2L gene, which targets both mitochondrial

and plastid PPO isoforms. This mechanism is particularly distinctive because it involves an amino acid deletion rather than the more typical substitution found in target-site resistance.

Recent research by Burgos et al. [28] identified a novel G399A mutation in the PPO2 catalytic domain of *Amaranthus palmeri* that confers broad resistance to PPO-inhibiting herbicides. Computational modeling and biochemical assays revealed that this glycine-to-alanine substitution creates steric hindrance, reducing herbicide binding affinity. Although less prevalent in field populations than the  $\Delta$ G210 mutation, G399A endows significant cross-resistance to multiple herbicide classes, including diphenylethers and triazolinones.

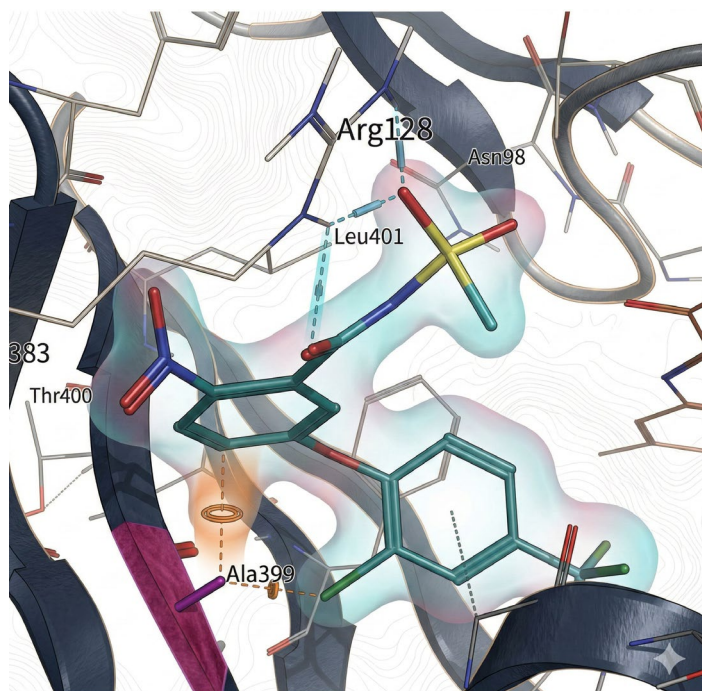


**Figure 4.** Position of the G399A mutation relative to the predicted binding mode of fomesafen. Fomesafen (cyan) was modeled into the binding-site of a homology model of a PPO2 protein sequence with G399A (gray) mutation. The alanine mutation is shown in pink.[28].

The engineering of crops resistant to PPO inhibitors has recently emerged as a focal point of intense scientific inquiry[1,29,30]. Research strategies have primarily centered on traditional tissue culture methodologies, the manipulation of co-factor expression for protoporphyrin IX-binding subunit proteins, and the deliberate overproduction of the endogenous plant PPO gene. To date, successful instances of herbicide tolerance have been documented in several cultivars, including rice, maize, tomato, tobacco, and soybean [25], with resistance levels spanning a broad spectrum from 2-fold to 1,000-fold.

Owing to the structural heterogeneity inherent in this herbicide class, the advancement of resistance technologies does not rely upon a solitary herbicide or a specific mutant gene. For instance, investigative efforts have explored herbicide-clearance mechanisms, such as chelatase-based approaches and the utilization of P-450 monooxygenases [31]. While the P-450 monooxygenase pathway holds promise for developing herbicide-resistant germplasm, its application to PPO-targeting chemistries faces a significant hurdle: the rapid physiological onset of these herbicides. Consequently, standard metabolic detoxification may be insufficiently fast to counteract such rapid-acting compounds. To address this, future engineering must prioritize P-450 monooxygenases characterized by exceptional catalytic efficiency and the versatile capacity to metabolize a diverse array of PPO inhibitor structures.

#### 4. Quantitative Structure-Activity Relationships of PPO Inhibitors

Following the patenting of oxadiazon and chlorophthalim in the early 1970s, a vast array of molecules has been synthesized and scrutinized for their herbicidal efficacy and PPO inhibitory

potential. To elucidate the underlying interaction mechanisms and streamline structural refinement, various Quantitative Structure-Activity Relationship (QSAR) models have been established[32]. A comprehensive synthesis of these QSAR advancements was provided by Fujita et al.[33], covering diverse chemical families such as thiadiazoles, diphenylethers, *N*-phenylphthalimides, and various *N*-phenyl-substituted heterocycles.

Notably, the predictive accuracy and robustness of a QSAR equation are fundamentally contingent upon the strategic selection of molecular descriptors. A prominent case in point is the *N*-phenyltriazolinone class, a significant group of PPO inhibitors pioneered by researchers at the FMC Corporation. This category includes key commercial agents such as sulfentrazone, a pre-emergent herbicide for soybean crops, and carfentrazone-ethyl, utilized for post-emergent weed control in cereals. Theodoridis and colleagues [13] conducted a targeted QSAR evaluation on a library of 1-substitutedphenyl-4H-1,2,4-triazolin-5-ones, utilizing hydroponic cucumber seedling assays to measure biological potency. The study investigated the correlation between herbicidal activity  $pI_{50}$  and two primary physicochemical parameters: the hydrophobicity constant  $\pi$  and the STERIMOL steric term  $B_1$ . Specifically, fourteen derivatives featuring substituents at the  $R_2$  position (position 5) of the phenyl ring were analyzed using equation (1):

$$pI_{50} = 7.02(\pm 2.351)B_1 - 0.18(\pm 0.045)\pi^2 - 2.57(\pm 0.775)B_1^2 + 2.51 \quad (1)$$

This model successfully explained 78% of the biological variance ( $r^2 = 0.78$ ), suggesting that activity reaches a peak when  $B_1 = 1.35$  and  $\pi = 0.02$ . Furthermore, greenhouse pre-emergence activity was shown to correlate well with these in-vitro results when hydrophobicity was factored in, explaining why certain hydrophilic groups, despite having lower intrinsic  $pI_{50}$  values, exhibit excellent whole-plant efficacy due to enhanced soil/water partitioning and root uptake. Conversely, substitutions at the 4-position proved more complex, requiring multiple models depending on whether the 5-position was occupied, with chloro or 4-chlorobenzoyloxy groups generally providing optimal activity.

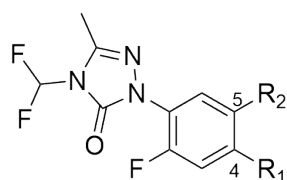


**Figure 5.** Structure and herbicidal activity of *N*-phenyl triazolinone derivatives.

However, divergent findings were later presented by Nicolaus et al.[34], whose subsequent QSAR modeling suggested that herbicidal efficacy was predominantly governed by substituent hydrophobicity rather than steric factors. These early computational efforts were constrained by their reliance on semiempirical electronic descriptors or basic physicochemical parameters, which typically focused on variations in the *N*-phenyl moiety while keeping the imine structure constant.

Electronic structure theory has evolved into an indispensable and potent instrument for the estimation of a broad array of molecular attributes, encompassing geometric configurations, energetics, chemical reactivity, and spectroscopic profiles. Among these methodologies, Density Functional Theory (DFT) stands out as a robust computational framework that effectively balances moderate resource expenditure with reliable precision. Consequently, it has been extensively utilized to probe the intricate electronic landscapes of molecular architectures, which are fundamental to understanding the binding dynamics between ligands and receptors.

A pioneering illustration of this application is the research conducted by Xi et al. [35], who introduced the inaugural quantum-chemical descriptor specifically designed to quantify steric effects. By modeling the volumetric distribution of the electron cloud via DFT simulations, they established a QSAR model with exceptional predictive fidelity for 35 sulfonylurea derivatives. It is significant to highlight that, while a multitude of quantum-chemical parameters had already been successfully integrated into QSAR frameworks, a dedicated theoretical metric for representing spatial hindrance had remained elusive until this development.

Zhang and colleagues [36] broadened the utility of the DFT-QSAR framework by applying it to the prediction of bioactive molecular arrangements. Their investigation concentrated on a library of cyclic imide analogs, for which three independent QSAR models were constructed, each corresponding to a distinct equilibrium conformation characterized via DFT descriptors.

Building upon these foundational SAR principles and other pioneering works [37,38], recent research[39] has applied Multivariate Image Analysis (MIA) to model the inhibitory activity of a diverse set of 61 benzothiazole derivatives (**Figure**). This advanced methodology encodes specific atomic properties—namely, Pauling's electronegativity ( $\epsilon$ ), van der Waals radii ( $r_{vdw}$ ), and their ratio ( $r_{vdw}/\epsilon$ )—directly into color-coded 2D chemical images. By utilizing a genetic algorithm to select the most relevant descriptors, researchers constructed highly robust Multiple Linear Regression (MLR) models for rapid activity prediction. For instance, the MLR model based on the  $r_{vdw}/\epsilon$  ratio is defined by the equation:

$$\begin{aligned}
 pK_i = & 12.7253(\pm 1.3219) + 0.0029(\pm 0.0014) \times MIA(r_{vdw}/\epsilon)5574 \\
 & + 0.0013(\pm 0.0003) \times MIA(r_{vdw}/\epsilon)9348 \\
 & + 0.0011(\pm 0.0002) \times MIA(r_{vdw}/\epsilon)5561 \\
 & - 0.0171(\pm 0.0036) \times MIA(r_{vdw}/\epsilon)6022 \\
 & + 0.0006(\pm 0.0003) \times MIA(r_{vdw}/\epsilon)2692
 \end{aligned}
 \tag{2}$$

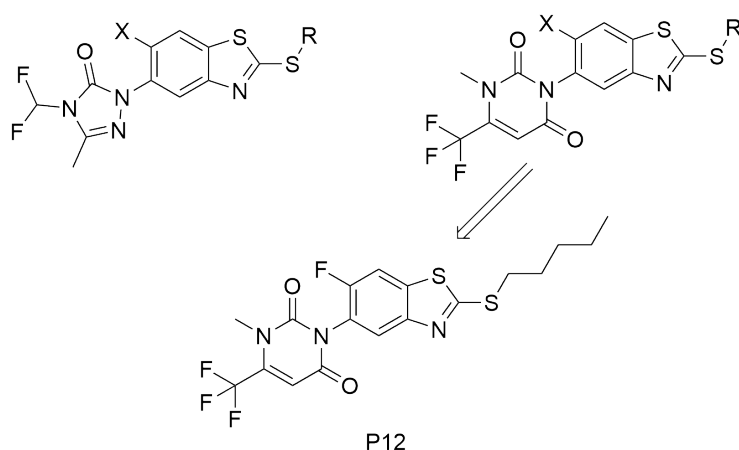


**Figure 6.** benzothiazole derivatives and the lead compound P12.

These MLR models, alongside complementary Partial Least-Squares (PLS) models, demonstrated exceptional statistical reliability, achieving correlation coefficients ( $r^2$ ) between 0.85 and 0.88, cross-validation scores ( $q^2$ ) of 0.75 to 0.83, and external predictive abilities ( $r^2_{pred}$ ) ranging from 0.77 to 0.86. (**Table 1**)

**Table 1.** The robust and predictive coefficients for MLR models.

Model Descriptor Type	Fitting( $r^2$ )	Cross-validation( $q^2$ )	External Prediction( $r^2_{pred}$ )
$r_{vdw}$	0.865	0.808	0.818
$\epsilon$	0.861	0.792	0.866
$r_{vdw}/\epsilon$	0.872	0.827	0.775

The structural insights derived from these MIA-QSAR contour maps and variable importance in projection (VIP) scores clearly identified critical regions for molecular optimization. Specifically, highly electronegative halogens like fluorine at the benzothiazole's X position significantly enhance binding affinity compared to chlorine or bromine. Additionally, incorporating longer alkyl chains at the R position improves hydrophobic interactions within the PPO active site. Leveraging these computational insights, a novel lead compound named P12 (**Figure**) was conceptualized. P12 features a pyrimidine heterocycle coupled with a pentyl chain, yielding a predicted activity ( $pK_i =$

7.93) that rivals the most potent known derivatives. Crucially, P12 boasts a calculated lipophilicity ( $\log P = 5.45$ ) substantially higher than that of commercial standards like sulfentrazone ( $\log P = 4.55$ ). This elevated lipophilicity not only implies improved leaf membrane permeation for post-emergence efficacy but also suggests a lower potential for environmental leaching, firmly establishing MIA-QSAR as a powerful paradigm for discovering the next generation of safe and effective agricultural herbicides.

Notably, the configuration indicated by the DFT-QSAR approach demonstrated exceptional structural alignment with the validated bioactive form. Consequently, this methodology serves as a streamlined alternative for determining the bioactive orientations of small molecules, proving particularly advantageous in scenarios where the tertiary structure of the target protein remains uncharacterized. This synergy between quantum mechanical calculations and quantitative structure-activity modeling significantly pushes the traditional boundaries of classical QSAR disciplines.

The preceding evidence underscores those descriptors derived from DFT yield predictive models with higher accuracy than those based on semiempirical methods or traditional physicochemical parameters. A particularly salient advantage of the DFT-QSAR framework is its ability to resolve the bioactive conformations of small molecules.

Conventionally, determining such conformations has relied on techniques like molecular dynamics (MD) simulations, nuclear magnetic resonance (NMR), and X-ray crystallography. However, these methodologies are frequently impeded by significant limitations, including prohibitive hardware costs, the logistical difficulty of acquiring target enzymes, and extensive time requirements. Crucially, the binding domains for many agrochemicals remain unidentified, rendering the experimental determination of their bioactive configurations nearly impossible. While QSAR analysis has solidified its status as a premier strategy for lead compound optimization and rational drug design, its application as a tool for analyzing bioactive conformations represents a relatively nascent frontier in the field.

## 5. The Recent Evolution of PPO Inhibitors

The distinct attributes associated with PPO-targeting herbicides have garnered significant interest from the global agrochemical community. Over the past ten years, substantial research endeavors have been directed toward the development of novel PPO inhibitors, leading to the identification of several noteworthy candidates that exhibit exceptional herbicidal potency.

The protoporphyrinogen-IX molecule exhibits a bipartite architecture dictated by its pyrrole ring substituents. This structure is characterized by a distinct lipophilic domain on one side, while the opposing side, bearing the propionic acid side chains, presents a significantly more hydrophilic profile. Although it was traditionally assumed that herbicides compete with the substrate by mimicking only two of its pyrrole rings, a major advancement occurred with the design of an inhibitor specifically engineered to replicate the spatial arrangement of the three rings[40], but not commercially launched to date.[11]

Beyond the triazolinone framework, various other heterocyclic scaffolds were extensively explored. Following the recognition of phenyluracils' herbicidal potential in the late 1980s, researchers successfully substituted the triazolinone moiety with a dihydropyrimidine-2,4-dione ring, establishing an entirely new class of phytotoxic agents [41]. A critical refinement in this series was the introduction of a trifluoromethyl group at the 6-position of the ring, which substantially enhanced biological potency. This optimization trajectory eventually led to the commercialization of four pivotal herbicides: flupropacil, benzfendizone, butafenacil, and saflufenacil[42](see **Figure** ).

Among these uracil-based compounds, saflufenacil has been registered as a highly effective selective herbicide for broadleaf weed management. It is versatile enough for both pre-emergence and post-emergence regimes across several key crops—including cotton, sunflowers, and soybeans—as well as for use in non-agricultural and fallow environments. Notably, saflufenacil demonstrates exceptional efficacy, providing a robust solution for controlling weed populations that have evolved resistance to glyphosate and AHAS-inhibiting chemistries.

Given their extensive weed-control profile, novel uracil-centered PPO inhibitors serve as compelling templates for scaffold hopping and isosteric investigations aimed at discovering new lead

motifs to manage resistant biotypes, which have moved beyond classical templates toward "resistance-breaking" architectures and pivoted toward increased structural complexity. Such as from traditional Two-Ring to Three-Ring architectures, Bioisosteric Side-Chain Replacement.

The first successfully commercialized uracil-centered herbicide with a two-ring system after saflufenacil is tiafenacil (**Figure**, compound 1). Studies[43] have elucidated the biochemical and physiological mode of action of tiafenacil. In vitro assays utilizing recombinant PPO enzymes from diverse plant species, including amaranth, soybean, arabidopsis, and rapeseed, demonstrated that tiafenacil possesses a highly potent binding affinity, with half-maximal inhibitory concentration  $IC_{50}$  values ranging narrowly from 22 to 28 nM. This high level of enzymatic inhibition is comparable to other highly active pyrimidinediones like saflufenacil and butafenacil, as well as the *N*-phenylphthalimide herbicide flumioxazin. Furthermore, tiafenacil proved to be significantly more efficient than traditional diphenyl ether (DPE) herbicides, exhibiting 3- to 134-fold lower  $IC_{50}$  values compared to fomesafen, oxyfluorfen, and acifluorfen.

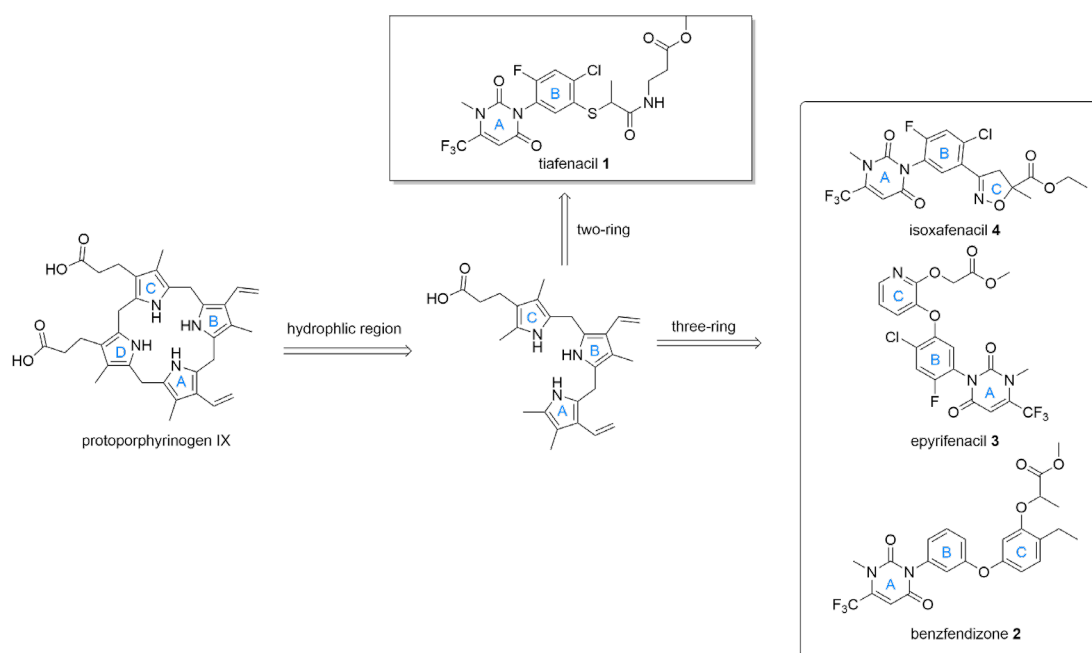


**Figure 7.** Novel uracil-centered PPO inhibitors with two-ring or three-ring.

The physiological consequences of this PPO inhibition follow a robust, light-dependent mechanism. When plant tissues are treated with tiafenacil in the dark, the enzymatic blockade leads to a marked accumulation of protoporphyrin IX. Upon subsequent exposure to light, this accumulation triggers a severe chain reaction of cellular damage. This oxidative stress is quantitatively confirmed by a rapid decrease in the Fv/Fm values of chlorophyll fluorescence, indicating compromised photosystem II efficiency, alongside a simultaneous increase in malondialdehyde (MDA) content, which serves as a biological marker for extensive lipid peroxidation and membrane disruption. As a result of this rapid structural degradation, tiafenacil acts as a highly effective, broad-spectrum herbicide capable of controlling both dicotyledonous and monocotyledonous plants at applied concentrations between 1 and 50  $\mu$ M. While dicot weeds like velvetleaf and amaranth are extremely sensitive and face lethal desiccation at doses as low as 1 to 5  $\mu$ M, monocots such as barnyardgrass and rice show slightly higher natural tolerance but are still effectively controlled at higher concentrations.

The recent publication by Sada et al. [44] introduces epyrifenacil (**Figure**, compound 3), a novel herbicide developed by Sumitomo Chemical that represents a significant evolution in the pyrimidinedione class of PPOs. Epyrifenacil is characterized by a unique three-ring structure that incorporates a pyridine ring. Unlike traditional contact-based PPO inhibitors, epyrifenacil exhibits exceptional systemic activity. Upon absorption, it is rapidly converted into an active acid metabolite that translocates efficiently through the plant's phloem in both basipetal and acropetal directions.

This systemic movement allows for the effective control of a broad spectrum of both broadleaf and grass weeds at exceptionally low application rates, such as 20 g a.i. ha<sup>-1</sup>. Furthermore, the herbicide demonstrates significant efficacy against weed biotypes that have evolved target-site resistance to existing PPO inhibitors, successfully controlling problematic species like Palmer amaranth carrying the  $\Delta G_{210}$ , Arg128Gly, or Gly399Ala mutations. In addition to its potent broad-spectrum and systemic herbicidal activity, epyrifenacil possesses an extremely low vapor pressure, which minimizes the risk of off-target drift and ensures the safety of adjacent sensitive crops.

To address the limitations of traditional PPOs, which typically exhibit weaker control over grassy weeds, researchers[45] designed a novel class of uracil-isoxazoline derivatives by integrating the highly active uracil scaffold of saflufenacil with an isoxazoline moiety. Utilizing the intermediate derivatization method, a series of nineteen new compounds were synthesized and evaluated for their herbicidal efficacy. Structure-activity relationship (SAR) analysis revealed that an ethyl substituent paired with a methyl group (identified as compound **4**, **Figure**) provided the optimal configuration for broad-spectrum activity. This optimized derivative demonstrated exceptional post-emergence activity at application rates as low as 7.5 g/ha, effectively controlling both broadleaf weeds and notoriously difficult grassy weeds, significantly outperforming saflufenacil on the latter. Furthermore, the compound exhibited potent efficacy against glyphosate-resistant biotypes, including *Conyza canadensis* and *Eleusine indica*, and produced a remarkable synergistic effect when applied in combination with glyphosate, highlighting its significant potential as a next-generation PPO-inhibiting herbicide for broad-spectrum weed management. Zhen Xi et al.[37,38,46-48] also developed a series of compounds via the "intermediate derivatization method," including *N*-Phenylaminomethylthioacetylpyrimidine-2,4-diones, *N*-Phenylisoxazoline-thiadiazolo[3,4-*a*]pyridazine, and others, but no commercialization has been reported to date.

Alnafta et al.[49] developed a series of novel uracil-based PPOs. The research leveraged scaffold hopping and bioisosteric replacement strategies, focusing specifically on the structural diversification of the side chains found in established inhibitors like tiafenacil and epyrifenacil. By utilizing molecular modeling based on a wild-type *Amaranthus tuberculatus* crystal structure, the authors designed and synthesized unprecedented side-chain motifs, including thioisoxazolines, thiolactams, and thioacrylamides. Experimental results indicate that isoxazoline-based derivatives provide effective control over resistant *Amaranthus* populations. Furthermore, the introduction of a thioacrylamide side chain in represents a significant breakthrough, affording exceptional efficacy against resistant monocotyledonous weeds like ryegrass (*Lolium* spp.) and black-grass (*Alopecurus myosuroides*). These advancements not only broaden the herbicidal spectrum but also offer improved crop safety in corn and wheat, illustrating that bioisosteric refinement is a pivotal tool for sustaining the utility of the PPO-inhibitor class.

Besides the commercialized and upcoming molecules mentioned above, researchers[50] have also developed other molecules through active substructure linking and bioisosterism replacement strategies to design a novel series of 47 tetrahydrophthalimide derivatives incorporating oxadiazole and thiadiazole moieties. By substituting these heterocycles at the 5-position of the *N*-phthalimide benzene ring, the study identified a compound featuring a 1,3,4-oxadiazole ring as a highly potent lead structure. In vitro assays demonstrated that this compound possesses an exceptional binding affinity for *Nicotiana tabacum* PPO (NtPPO) with a  $K_i$  of 9.05 nM, significantly outperforming the commercial standard flumiclorac-pentyl ( $K_i = 46.02$  nM). Molecular docking and molecular dynamics simulations revealed that this enhanced affinity is driven by strong hydrogen bonding with the Arg98 (2.9 Å) and Ser235 (2.7 Å) residues, alongside stable  $\pi$ - $\pi$  stacking with Phe392 and  $\pi$ -conjugation with Leu356 and Leu372.

## 6. Conclusions

In summary, more than six decades of research have established PPO as a key target for herbicide discovery. PPO-inhibiting herbicides possess favorable traits, being environmentally friendly, yet improper application can lead to crop injury. Although a wide array of PPO inhibitors have been commercialized, the escalating evolution of weed resistance continues to fuel interest in developing next-generation PPO-inhibiting herbicides. To advance the design of novel inhibitors,

beyond exploiting known knowledge to refine chemical structures via innovative pharmacophores such as scaffold hopping, bioisosteric replacement, and pro-herbicide activation, fundamental questions concerning PPO structure and function must still be addressed. These include elucidating the detailed catalytic mechanism of the enzyme, the mode of substrate binding, and the process of product release. Moreover, all current PPO inhibitors function through competitive inhibition; exploring non-competitive inhibition represents a promising alternative strategy.

**Acknowledgments:** We appreciate the financial support from the Doctoral Science Foundation of Xinjiang Second Medical College (XGYK2025-102) and the Karamay Science and Technology Plan Project (2025BA0090).

**Conflicts of Interest:** The authors declare no conflicts of interest.

## Abbreviations

The following abbreviations are used in this manuscript:

bsPPO	Bacillus subtilis PPO
DFT	Density Functional Theory
FAD	flavin adenine dinucleotide
hPPO	human ortholog PPO
INH	inhibitor
MD	molecular dynamics
MDA	malondialdehyde
MIA	Multivariate Image Analysis
MLR	Multiple Linear Regression
mtPPO	mitochondrial PPO2
mxPPO	Myxococcus xanthus PPO
NMR	nuclear magnetic resonance
PDT	photodynamic therapy
PLS	Partial Least-Squares
PPO	protoporphyrinogen oxidase
QSARs	quantitative structure-activity relationships
SAR	structure-activity relationships
VIP	Variable Importance in Projection
VP	variegated porphyria

## References

1. Barker, A.L.; Pawlak, J.; Duke, S.O.; Beffa, R.; Tranel, P.J.; Wuerffel, J.; Young, B.; Porri, A.; Liebl, R.; Aponte, R.; et al. Discovery, mode of action, resistance mechanisms, and plan of action for sustainable use of Group 14 herbicides. *Weed Science* **2023**, *71*, 173-188, doi:10.1017/wsc.2023.15.
2. Lermontova, I.; Kruse, E.; Mock, H.P.; Grimm, B. Cloning and characterization of a plastidal and a mitochondrial isoform of tobacco protoporphyrinogen IX oxidase. *Proc Natl Acad Sci U S A* **1997**, *94*, 8895-8900, doi:10.1073/pnas.94.16.8895.
3. Brenner, D.A.; Bloomer, J.R. The enzymatic defect in variegate prophyria. Studies with human cultured skin fibroblasts. *N Engl J Med* **1980**, *302*, 765-769, doi:10.1056/nejm198004033021401.
4. MEISSNER, P.N.; DAY, R.S.; MOORE, M.R.; DISLER, P.B.; HARLEY, E. Protoporphyrinogen oxidase and porphobilinogen deaminase in variegate porphyria. *European Journal of Clinical Investigation* **1986**, *16*, 257-261, doi:https://doi.org/10.1111/j.1365-2362.1986.tb01339.x.
5. Nordmann, Y.; Puy, H. Human hereditary hepatic porphyrias. *Clin Chim Acta* **2002**, *325*, 17-37, doi:10.1016/s0009-8981(02)00276-0.
6. Frank, J.; Christiano, A.M. Variegate porphyria: past, present and future. *Skin Pharmacol Appl Skin Physiol* **1998**, *11*, 310-320, doi:10.1159/000029854.
7. Maneli, M.H.; Corrigall, A.V.; Klump, H.H.; Davids, L.M.; Kirsch, R.E.; Meissner, P.N. Kinetic and physical characterisation of recombinant wild-type and mutant human protoporphyrinogen oxidases. *Biochim Biophys Acta* **2003**, *1650*, 10-21, doi:10.1016/s1570-9639(03)00186-9.

8. Georgakoudi, I.; Keng, P.C.; Foster, T.H. Hypoxia significantly reduces aminolaevulinic acid-induced protoporphyrin IX synthesis in EMT6 cells. *British Journal of Cancer* **1999**, *79*, 1372-1377, doi:10.1038/sj.bjc.6690220.
9. Halling, B.P.; Yuhas, D.A.; Fingar, V.F.; Winkelmann, J.W. Protoporphyrinogen Oxidase Inhibitors for Tumor Therapy. In *Porphyric Pesticides*; ACS Symposium Series; American Chemical Society: 1994; Volume 559, pp. 280-290.
10. Hao, G.F.; Zuo, Y.; Yang, S.G.; Yang, G.F. Protoporphyrinogen oxidase inhibitor: an ideal target for herbicide discovery. *Chimia (Aarau)* **2011**, *65*, 961-969, doi:10.2533/chimia.2011.961.
11. Yan, Y.; Geng, W.; Chen, C.; Yan, K.; Gan, X. Novel Phenylpyrazole Derivatives Containing Carbonic Ester Moieties as Protoporphyrinogen IX Oxidase Inhibitors. *Journal of Agricultural and Food Chemistry* **2025**, *73*, 22150-22161, doi:10.1021/acs.jafc.5c02008.
12. Gitsopoulos, T.K.; Froud-Williams, R.J. Effects of oxadiargyl on direct-seeded rice and *Echinochloa crus-galli* under aerobic and anaerobic conditions. *Weed Research* **2004**, *44*, 329-334, doi:10.1111/j.1365-3180.2004.00407.x.
13. Theodoridis, G. Structure-Activity Relationships of Herbicidal Aryltriazolinones. *Pesticide Science* **1997**, *50*, 283-290, doi:https://doi.org/10.1002/(SICI)1096-9063(199708)50:4<283::AID-PS600>3.0.CO;2-L.
14. Ohta, H.; Jikihara, T.; Wakabayashi, K.; Fujita, T. Quantitative structure-activity study of herbicidal N-aryl-3,4,5,6-tetrahydrophthalimides and related cyclic imides. *Pesticide Biochemistry and Physiology* **1980**, *14*, 153-160, doi:https://doi.org/10.1016/0048-3575(80)90106-6.
15. Theodoridis, G.; Liebl, R.; Zagar, C. Protoporphyrinogen IX Oxidase Inhibitors. In *Modern Crop Protection Compounds*; 2011; pp. 163-195.
16. Murphy, B.P.; Tranel, P.J. Target-Site Mutations Conferring Herbicide Resistance. *Plants* **2019**, *8*, 382.
17. Lyga, J.W.; Patera, R.M.; Theodoridis, G.; Halling, B.P.; Hotzman, F.W.; Plummer, M.J. Synthesis and quantitative structure-activity relationships of herbicidal N-(2-fluoro-5-methoxyphenyl)-3,4,5,6-tetrahydrophthalimides. *Journal of Agricultural and Food Chemistry* **1991**, *39*, 1667-1673, doi:10.1021/jf00009a025.
18. Simmons, K.A.; Dixon, J.A.; Halling, B.P.; Plummer, E.L.; Plummer, M.J.; Tymonko, J.M.; Schmidt, R.J.; Wyle, M.J.; Webster, C.A.; et al. Synthesis and activity optimization of herbicidal substituted 4-aryl-1,2,4-triazole-5(1H)-thiones. *Journal of Agricultural and Food Chemistry* **1992**, *40*, 297-305, doi:10.1021/jf00014a027.
19. Brzezowski, P.; Ksas, B.; Havaux, M.; Grimm, B.; Chazaux, M.; Peltier, G.; Johnson, X.; Alric, J. The function of PROTOPORPHYRINOGEN IX OXIDASE in chlorophyll biosynthesis requires oxidised plastoquinone in *Chlamydomonas reinhardtii*. *Communications Biology* **2019**, *2*, 159, doi:10.1038/s42003-019-0395-5.
20. Dan Hess, F. Light-dependent herbicides: an overview. *Weed Science* **2000**, *48*, 160-170, doi:10.1614/0043-1745(2000)048[0160:LDHAO]2.0.CO;2.
21. Koch, M.; Breithaupt, C.; Kiefersauer, R.; Freigang, J.; Huber, R.; Messerschmidt, A. Crystal structure of protoporphyrinogen IX oxidase: a key enzyme in haem and chlorophyll biosynthesis. *The EMBO Journal* **2004**, *23*, 1720-1728, doi:10.1038/sj.emboj.7600189.
22. Corradi, H.R.; Corrigan, A.V.; Boix, E.; Mohan, C.G.; Sturrock, E.D.; Meissner, P.N.; Acharya, K.R. Crystal structure of protoporphyrinogen oxidase from *Myxococcus xanthus* and its complex with the inhibitor acifluorfen. *J Biol Chem* **2006**, *281*, 38625-38633, doi:10.1074/jbc.M606640200.
23. Qin, X.; Sun, L.; Wen, X.; Yang, X.; Tan, Y.; Jin, H.; Cao, Q.; Zhou, W.; Xi, Z.; Shen, Y. Structural insight into unique properties of protoporphyrinogen oxidase from *Bacillus subtilis*. *J Struct Biol* **2010**, *170*, 76-82, doi:10.1016/j.jsb.2009.11.012.
24. Qin, X.; Tan, Y.; Wang, L.; Wang, Z.; Wang, B.; Wen, X.; Yang, G.; Xi, Z.; Shen, Y. Structural insight into human variegate porphyria disease. *Faseb j* **2011**, *25*, 653-664, doi:10.1096/fj.10-170811.
25. Burgos, N.R.; Tranel, P.J.; Streibig, J.C.; Davis, V.M.; Shaner, D.; Norsworthy, J.K.; Ritz, C. Review: Confirmation of Resistance to Herbicides and Evaluation of Resistance Levels. *Weed Science* **2013**, *61*, 4-20, doi:10.1614/WS-D-12-00032.1.
26. Owen, M.D.; Zelaya, I.A. Herbicide-resistant crops and weed resistance to herbicides. *Pest Management Science* **2005**, *61*, 301-311, doi:https://doi.org/10.1002/ps.1015.

27. Patzoldt, W.L.; Hager, A.G.; McCormick, J.S.; Tranel, P.J. A codon deletion confers resistance to herbicides inhibiting protoporphyrinogen oxidase. *Proc Natl Acad Sci U S A* **2006**, *103*, 12329-12334, doi:10.1073/pnas.0603137103.
28. Rangani, G.; Salas-Perez, R.A.; Aponte, R.A.; Knapp, M.; Craig, I.R.; Mietzner, T.; Langaro, A.C.; Noguera, M.M.; Porri, A.; Roma-Burgos, N. A Novel Single-Site Mutation in the Catalytic Domain of Protoporphyrinogen Oxidase IX (PPO) Confers Resistance to PPO-Inhibiting Herbicides. *Frontiers in Plant Science* **2019**, Volume 10 - 2019, doi:10.3389/fpls.2019.00568.
29. Li, X.; Nicholl, D. Development of PPO inhibitor-resistant cultures and crops. *Pest Management Science* **2005**, *61*, 277-285, doi:https://doi.org/10.1002/ps.1011.
30. Koch, A.C.; Ramgareeb, S.; Snyman, S.J.; Watt, M.P.; Rutherford, R.S. Pursuing herbicide tolerance in sugarcane: screening germplasm and induction through mutagenesis. 2009.
31. Werck-Reichhart, D.; Feyereisen, R. Cytochromes P450: a success story. *Genome Biol* **2000**, *1*, Reviews3003, doi:10.1186/gb-2000-1-6-reviews3003.
32. Tropsha, A. Best Practices for QSAR Model Development, Validation, and Exploitation. *Molecular Informatics* **2010**, *29*, 476-488, doi:https://doi.org/10.1002/minf.201000061.
33. Fujita, T.; Nakayama, A. Structure-Activity Relationship and Molecular Design of Peroxidizing Herbicides with Cyclic Imide Structures and Their Relatives. In *Peroxidizing Herbicides*, Böger, P., Wakabayashi, K., Eds.; Springer Berlin Heidelberg: Berlin, Heidelberg, 1999; pp. 91-139.
34. Nicolaus, B.; Sandmann, G.; Böger, P. Molecular Aspects of Herbicide Action on Protoporphyrinogen Oxidase. **1993**, *48*, 326-333, doi:doi:10.1515/znc-1993-3-434.
35. Xi, Z.; Yu, Z.; Niu, C.; Ban, S.; Yang, G. Development of a general quantum-chemical descriptor for steric effects: Density functional theory based QSAR study of herbicidal sulfonylurea analogues. *Journal of Computational Chemistry* **2006**, *27*, 1571-1576, doi:https://doi.org/10.1002/jcc.20464.
36. Zhang, L.; Wan, J.; Yang, G. A DFT-based QSARs study of protoporphyrinogen oxidase inhibitors: phenyl triazolinones. *Bioorganic & Medicinal Chemistry* **2004**, *12*, 6183-6191, doi:https://doi.org/10.1016/j.bmc.2004.08.046.
37. Zheng, B.-F.; Zuo, Y.; Huang, G.-Y.; Wang, Z.-Z.; Ma, J.-Y.; Wu, Q.-Y.; Yang, G.-F. Synthesis and Biological Activity Evaluation of Benzoxazinone-Pyrimidinedione Hybrids as Potent Protoporphyrinogen IX Oxidase Inhibitor. *Journal of Agricultural and Food Chemistry* **2023**, *71*, 14221-14231, doi:10.1021/acs.jafc.3c03593.
38. Zheng, B.-F.; Wang, Z.-Z.; Dong, J.; Ma, J.-Y.; Zuo, Y.; Wu, Q.-Y.; Yang, G.-F. Discovery of a Subnanomolar Inhibitor of Protoporphyrinogen IX Oxidase via Fragment-Based Virtual Screening. *Journal of Agricultural and Food Chemistry* **2023**, *71*, 8746-8756, doi:10.1021/acs.jafc.3c00168.
39. de Faria, A.C.; Mesquita, A.P.L.; da Cunha, E.F.F.; Freitas, M.P. Exploitation, QSAR, and Structure-Based Modeling of Benzothiazole Derivatives as Protoporphyrinogen Oxidase IX Inhibitors. *ACS Agricultural Science & Technology* **2026**, *6*, 229-243, doi:10.1021/acsagritech.5c00950.
40. Mattison, R.L.; Beffa, R.; Bojack, G.; Bollenbach-Wahl, B.; Dörnbrack, C.; Dorn, N.; Freigang, J.; Gatzweiler, E.; Getachew, R.; Hartfiel, C.; et al. Design, synthesis and screening of herbicidal activity for new phenyl pyrazole-based protoporphyrinogen oxidase-inhibitors (PPO) overcoming resistance issues. *Pest Management Science* **2023**, *79*, 2264-2280, doi:https://doi.org/10.1002/ps.7425.
41. Theodoridis, G.; Bahr, J.T.; Hotzman, F.W.; Saroj, S.; Suarez, D.P. New generation of protox-inhibiting herbicides. *Crop Protection* **2000**, *19*, 533-535, doi:https://doi.org/10.1016/S0261-2194(00)00069-7.
42. Maienfisch, P.; Koerber, K. Recent innovations in crop protection research. *Pest Management Science* **2025**, *81*, 2406-2418, doi:https://doi.org/10.1002/ps.8441.
43. Park, J.; Ahn, Y.O.; Nam, J.-W.; Hong, M.-K.; Song, N.; Kim, T.; Yu, G.-H.; Sung, S.-K. Biochemical and physiological mode of action of tiafenacil, a new protoporphyrinogen IX oxidase-inhibiting herbicide. *Pesticide Biochemistry and Physiology* **2018**, *152*, 38-44, doi:https://doi.org/10.1016/j.pestbp.2018.08.010.
44. Sada, Y.; Jin, Y.; Hikosaka, M.; Ido, K. Epyrifencil, a new systemic PPO-inhibiting herbicide for broad-spectrum weed control. *Pest Management Science* **2025**, *81*, 2463-2468, doi:https://doi.org/10.1002/ps.8244.
45. Yang, J.; Guan, A.; Wu, Q.; Cui, D.; Liu, C. Design, synthesis and herbicidal evaluation of novel uracil derivatives containing an isoxazoline moiety. *Pest Management Science* **2020**, *76*, 3395-3402, doi:https://doi.org/10.1002/ps.5970.

46. Wang, D.-W.; Liang, L.; Xue, Z.-Y.; Yu, S.-Y.; Zhang, R.-B.; Wang, X.; Xu, H.; Wen, X.; Xi, Z. Discovery of N-Phenylaminomethylthioacetylpyrimidine-2,4-diones as Protoporphyrinogen IX Oxidase Inhibitors through a Reaction Intermediate Derivation Approach. *Journal of Agricultural and Food Chemistry* **2021**, *69*, 4081-4092, doi:10.1021/acs.jafc.1c00796.
47. Zhang, R.-B.; Yu, S.-Y.; Liang, L.; Ismail, I.; Wang, D.-W.; Li, Y.-H.; Xu, H.; Wen, X.; Xi, Z. Design, Synthesis, and Molecular Mechanism Studies of N-Phenylisoxazoline-thiadiazolo[3,4-a]pyridazine Hybrids as Protoporphyrinogen IX Oxidase Inhibitors. *Journal of Agricultural and Food Chemistry* **2020**, *68*, 13672-13684, doi:10.1021/acs.jafc.0c05955.
48. Wang, D.-W.; Zhang, R.-B.; Yu, S.-Y.; Liang, L.; Ismail, I.; Li, Y.-H.; Xu, H.; Wen, X.; Xi, Z. Discovery of Novel N-Isoxazolinyphenyltriazinones as Promising Protoporphyrinogen IX Oxidase Inhibitors. *Journal of Agricultural and Food Chemistry* **2019**, *67*, 12382-12392, doi:10.1021/acs.jafc.9b04844.
49. Alnafta, N.; Beffa, R.; Bojack, G.; Bollenbach-Wahl, B.; Brant, N.Z.; Dörnbrack, C.; Dorn, N.; Freigang, J.; Gatzweiler, E.; Getachew, R.; et al. Designing New Protoporphyrinogen Oxidase-Inhibitors Carrying Potential Side Chain Isosteres to Enhance Crop Safety and Spectrum of Activity. *Journal of Agricultural and Food Chemistry* **2023**, *71*, 18270-18284, doi:10.1021/acs.jafc.3c01420.
50. Geng, W.; Zhang, Q.; Liu, L.; Tai, G.; Gan, X. Design, Synthesis, and Herbicidal Activity of Novel Tetrahydrophthalimide Derivatives Containing Oxadiazole/Thiadiazole Moieties. *Journal of Agricultural and Food Chemistry* **2024**, *72*, 17191-17199, doi:10.1021/acs.jafc.4c01389.

**Disclaimer/Publisher's Note:** The statements, opinions and data contained in all publications are solely those of the individual author(s) and contributor(s) and not of MDPI and/or the editor(s). MDPI and/or the editor(s) disclaim responsibility for any injury to people or property resulting from any ideas, methods, instructions or products referred to in the content.